CENTRE DE RECERCA MATEMÀTICA

This is a preprint of: *A wavefunction description of stochastic-mechanics tion: Fokker-Planck derivation, dissipastationary dynamics and numerical approximations*
Journal Information: *CRM Preprints*,
Author(s): P. Guerrero, J.L. López and J. Montejo-Gámez.
Volume, pages: *1-32*, DOI:[--]

Preprint núm. 1159
June 2013

# A wavefunction description of stochastic-mechanics Fokker-Planck dissipation: derivation, stationary dynamics and numerical approximations

P. Guerrero, J. L. López, J. Montejo–Gámez

# A WAVEFUNCTION DESCRIPTION OF STOCHASTIC-MECHANICS FOKKER-PLANCK DISSIPATION: DERIVATION, STATIONARY DYNAMICS AND NUMERICAL APPROXIMATIONS

PILAR GUERRERO, JOSÉ LUIS LÓPEZ, AND JESÚS MONTEJO–GÁMEZ

Abstract. A nonlinear Schrödinger equation describing how a quantum particle interacts with its surrounding reservoir is derived from the Wigner–Fokker–Planck equation (WFPE) via stochastic (Nelsonian) mechanical techniques. This model can be reduced just to a logarithmic Schrödinger equation (LSE) through a suitable gauge transformation that allows to explore its steady state dynamics and makes its mathematical and numerical analysis more tractable. The transient behaviour of the standard deviation from the mean position associated with its solutions is also studied numerically and compared with that stemming from the WFPE.

## 1. Introduction

The modeling of quantum dissipation has experienced a great impulse over recent years mainly due to the investigation of system+reservoir structures, which take into account energy transfer from the system to the environment (e.g. semiconductor devices with doped regions as reservoirs that inject electrons into the active regions). This aims to open quantum systems as the most common physical scenario [9], i.e. a particle ensemble interacting dissipatively with an idealized heat bath of harmonic oscillators, whose effect on the particle motion is typically described by the bath temperature and the friction parameter after tracing over the reservoir degrees of freedom.

One of the best accepted diffusion mechanisms in modern quantum mechanics is the Fokker–Planck scattering kernel when added to Wigner's equation. Remarkably, the Caldeira–Leggett master equation [4] has been succeedingly applied to model quantum Brownian motion in spite of its mathematical defficiencies, as it does not fit the Kossakowski–Lindblad form [22, 25] so as to guarantee positivity of the density matrix operator. The WFPE is the most general extension of the pioneering Caldeira–Legett master equation, which models the interaction of a quantum fermionic gas with a thermal bath subject to moderate/high temperatures:

$$\partial_t w + \xi \cdot \nabla_x w + \theta_V(w) = \mathcal{L}_{QFP}(w)\,, \tag{1}$$

CRM Preprint Series number 1159

with

$$\mathcal{L}_{QFP}(w) = \frac{D_{pp}}{m^2}\Delta_\xi w + 2\lambda\nabla_\xi\cdot(\xi w) + 2\frac{D_{pq}}{m}\nabla_x\cdot\nabla_\xi w + D_{qq}\Delta_x w\,, \tag{2}$$

where $w(t,x,\xi)$ is the quasiprobability Wigner distribution, as it may assume negative values. Here $x,\xi\in\mathbb{R}^N$ are the position and velocity coordinates of the electron gas, $t\geq 0$ is the time variable,

$$D_{pp} = 2m\lambda k_B T\,,\quad D_{pq} = \frac{\lambda\Omega\hbar^2}{6\pi k_B T}\,,\quad D_{qq} = \frac{\lambda\hbar^2}{6mk_B T} \tag{3}$$

are phenomenological constants related to electron–bath interactions, $\lambda$ is the friction coefficient, $\Omega$ the cut–off frequency of the oscillators conforming the thermal bath, $T$ the bath temperature, $m$ the effective mass of the particles, $k_B$ the Boltzmann constant, $\hbar$ the (reduced) Planck constant, and where

$$\theta_V(w)(t,x,\xi) = \frac{i}{(2\pi)^N}\int_{\mathbb{R}^{2N}}\delta V(t,x,\eta)\,w(t,x,\xi')\,e^{i(\xi'-\xi)\cdot\eta}\,d\xi'\,d\eta \tag{4}$$

is a pseudo–differential operator related to the external potential $V$ through the symbol

$$\delta V(t,x,\eta) = \frac{1}{\hbar}\left(V\left(t,x+\frac{\hbar}{2m}\eta\right) - V\left(t,x-\frac{\hbar}{2m}\eta\right)\right)\,. \tag{5}$$

In the presence of a purely Ohmic environment (namely, linear coupling in both system and environment coordinates), the WFPE comes out from the Liouville operator $\partial_t\rho = L[\rho]$ after Wignerization (see §2 in [1]), with

$$\begin{aligned} L[\rho] = &-\frac{i}{\hbar}\big(H_x - H_y\big)\rho - \lambda(x-y)\cdot(\nabla_x-\nabla_y)\rho \\ &+ \Big(D_{qq}|\nabla_x+\nabla_y|^2 - \frac{D_{pp}}{\hbar^2}|x-y|^2 - \frac{2i}{\hbar}D_{pq}(x-y)\cdot(\nabla_x+\nabla_y)\Big)\rho\,, \end{aligned}$$

where $H = -\frac{\hbar^2}{2m}\Delta_x + V(x)$ is the electron Hamiltonian ($H_x$ and $H_y$ denoting two copies of $H$ acting on the variables $x$ and $y$, respectively) and where $\rho$ is the (integral kernel of the) reduced density matrix operator, derived in [13] as the Markovian approximation of the originally non–Markovian evolution of the particles in the oscillator bath. Here, the parameters are as follows:

- (H1) The reservoir memory time $\Omega^{-1}$ is much smaller than the characteristic time scale of the particles;
- (H2) weak coupling: $\lambda \ll \Omega$, and
- (H3) medium/high temperatures: $\Omega \lesssim \frac{k_B T}{\hbar}$.

Notice that the Caldeira–Leggett model is obtained when $D_{pq} = D_{qq} = 0$ is assumed in the WFPE, that is, in the context of a high–temperatures regime. Other models belonging to the Kossakowski–Lindblad class were derived for example in [15] and [35].

Nevertheless, though many nonlinear corrections have been proposed up to now, quantum dissipative interactions are still far from being well understood (mainly in the Schrödinger picture), and still deeper insight on their mathematical modeling and physical interpretation is required. Our main purpose is to derive a multidimensional nonlinear Schrödinger equation of logarithmic type describing much the same effects as the WFPE. Following a Nelsonian procedure as in [32], we are led to the following equation

$$
\begin{aligned}
i\alpha\partial_t\Psi = & \left(-\frac{\alpha^2}{2m}\Delta_x + V\right)\Psi + \frac{\alpha^2}{\hbar^2}Q\Psi + \Lambda\log(n)\Psi \\
& + \alpha D_{qq}\left\{\frac{i}{2}\frac{\Delta_x n}{n} + \frac{m}{\hbar}\nabla_x\cdot\left(\frac{J_\Psi}{n}\right)\right\}\Psi\,,
\end{aligned} \tag{6}
$$

with $\alpha = 2mD_{qq}$ as the new action unit (see § 2.2 for a discussion),

$$
\Lambda := 2D_{pq} + \alpha\lambda\,, \tag{7}
$$

and

$$
\begin{aligned}
& n = |\Psi|^2\,, \quad J_\Psi = \frac{\hbar}{m}\mathrm{Im}\big(\overline{\Psi}\nabla_x\Psi\big)\,, \\
& Q = -\frac{\hbar^2}{2m}\frac{\Delta_x\sqrt{n}}{2\sqrt{n}} = -\frac{\hbar^2}{4m}\left(\frac{\Delta_x n}{n} - \frac{|\nabla_x n|^2}{2n^2}\right)
\end{aligned}
$$

denoting the probability and current densities and the quantum potential, respectively, where $\mathrm{Im}(z)$ stands for the imaginary part of the complex number $z$. After being gauged through the nonlinear transformation

$$
\Psi \longmapsto \Phi = \Psi\exp\left\{-\frac{i}{2}\log(n)\right\}\,,
$$

Eq. (6) can be simply shown to be reduced to the following (purely) LSE

$$
i\alpha\partial_t\Phi = \left(-\frac{\alpha^2}{2m}\Delta_x + V\right)\Phi + \Lambda\log(n)\Phi\,. \tag{8}
$$

We shall then simulate numerically the expected dispersive behaviour of Eq. (8) (that retain much the same macroscopic dynamics that Eq. (6), in the sense that $|\Phi|^2 = |\Psi|^2$) in order to compare it with the exact results stemming from the WFPE.

The structure of the paper is the following: In Section 2 we carry out the derivation of Eq. (6), starting from the WFPE, through Nelsonian stochastic mechanical techniques. In Section 3 its stationary dynamics is analyzed. Section 4 concerns the presentation of several simulations for the free particle and the harmonic oscillator cases, as well as comparisons with the exact results exhibited by the WFPE. Two appendices finally stand for the description of the adimensionalization process and of some remarkable features of the numerical method employed.

## 2. The wavefunction approach

In many mathematical and physical situations the Schrödinger picture of quantum mechanics is preferable to the Liouvillian representation, mainly for computational reasons. Indeed, the Wigner function is evaluated in the position–momentum space, which makes the subsequent numerical analysis certainly intricate. Even from an analytical viewpoint, though most PDE techniques are expected to be inhereted from kinetic theory, the fact that the probability distribution (i.e. the Wigner function) can assume negative values constitutes a serious drawback in making things rigorous. In any case, it seems convenient to have an equivalent' description of the dissipative Fokker–Planck mechanism, that has proved to give satisfactory results in both the Wigner and the quantum hydrodynamic formulations, in terms of the particle wavefunction.

Starting from the WFPE, we shall derive here below a nonlinear dissipative Schrödinger equation characterized in an essential way by the presence of a quantum correction of logarithmic type (already present in the literature since the seminal work by Bialynicki–Birula and Mycielski [3]) as well as of various other nonlinearities that fit the Doebner–Goldin diffusive structure [14]. This kind of models has been already dealt with in the literature, for instance in [26, 27, 28, 29]. As will be seen, this equation does retain the same macroscopic local density that the WFPE we started with. The derivation follows the fundamental lines of Nelsonian stochastic mechanics [32] combined with the Madelung theory [30].

### 2.1. Nelsonian approach to Wigner–Fokker–Planck hydrodynamics.

One of the main aspects of quantum–mechanical Fokker–Planck theories relies on the presence of a diffusion current stemming from the (nonzero) right–hand side of the continuity equation. In this case, the equation for the position density reads

$$\partial_t n + \nabla_x \cdot J = D_{qq}\Delta_x n\,, \tag{9}$$

which is of Fokker–Planck type. Here, we denoted

$$n = \int_{\mathbb{R}^N} w\, d\xi\,, \quad J = \int_{\mathbb{R}^N} \xi w\, d\xi \tag{10}$$

the position and current densities, respectively. This equation along with

$$\begin{aligned}\partial_t u + (u\cdot\nabla_x)u = &-\frac{1}{m}\nabla_x V - \frac{1}{n}\mathrm{div}_x(\mathbb{P}_u) - 2\lambda u - \frac{2D_{pq}}{m}\nabla_x \log(n)\\ &+ D_{qq}\Big(2\nabla_x \log(n)\cdot\nabla_x u + \Delta_x u\Big)\,,\end{aligned} \tag{11}$$

constitute the hydrodynamic system associated with the WFPE, where $u = \frac{J}{n}$ represents the fluid mean velocity and where

$$\mathbb{P}_u = \int_{\mathbb{R}^N} \xi\otimes\xi w\, d\xi - nu\otimes u$$

denotes the rank–2 stress tensor. Notice that the presence of the internal stress tensor $\mathbb{P}_u$ makes Eqs. (9) and (11) not to form a self–consistent system, so that we are firstly called to close it in a proper way.

The basic idea underlying our derivation consists of reinterpreting the continuity equation in terms of Nelsonian stochastic mechanics. This theory yields a quantum–mechanical description by means of classical probability densities for particles undergoing Brownian motion with diffusive interactions. In this spirit, the Schrödinger equation will arise from a suitable interpretation of the evolution of a classical particle subject to Brownian motion. Indeed, in our context it is assumed that the diffusive contributions observed in the formulation of the WFPE stem from Brownian motion as produced by the dissipative interaction between the electron gas and the thermal environment. Thus, the particle is subject to the action of forward and backward velocities $u_+$ and $u_- = u_+ - 2u_0$, respectively, entering the continuity equation as

$$\partial_t n + \nabla_x \cdot (n u_\pm) = \pm D_{qq} \Delta_x n \,. \tag{12}$$

Here,

$$u_o := D_{qq} \nabla_x \log(n) \tag{13}$$

is the so–called osmotic velocity associated with the diffusion governed by the coefficient $D_{qq}$, that sets the exact balance between the macroscopic and the diffusion currents (see formula (14) below). Summing up both forward and backward contributions in Eq. (12) and introducing the current mean velocity

$$v := \frac{1}{2}(u_+ + u_-) = u_+ - u_o \,, \tag{14}$$

it is a simple matter to check that the standard continuity equation of quantum mechanics, namely

$$\partial_t n + \nabla_x \cdot (n v) = 0 \,, \tag{15}$$

is recovered. By defining the mean backward derivative of the forward velocity as

$$\mathcal{D}_- u_+ := \partial_t u_+ + u_- \cdot \nabla_x u_+ - D_{qq} \Delta_x u_+ \,,$$

the velocity equation can be rewritten for $u_+$ as

$$\mathcal{D}_- u_+ = -\frac{1}{m} \nabla_x V - \frac{\mathrm{div}_x(\mathbb{P}_{u_+})}{n} - 2\lambda u_+ - \frac{2D_{pq}}{m} \nabla_x \log(n) \,. \tag{16}$$

We now perform time inversion according to the following rules [18]

$$t \longmapsto -t \,, \quad \partial_t \longmapsto -\partial_t \,, \quad u_\pm, v \longmapsto -u_\mp, -v \,, \quad \mathcal{D}_\pm \longmapsto -\mathcal{D}_\mp \,.$$

Since $\mathbb{P}_{u_+}$ is a dynamic characteristic of motion, its divergence changes sign under time inversion. Accordingly, Eq. (16) becomes

$$\mathcal{D}_+ u_- = -\frac{1}{m} \nabla_x V + \frac{\mathrm{div}_x(\mathbb{P}_{u_+})}{n} + 2\lambda u_- - \frac{2D_{pq}}{m} \nabla_x \log(n) \,, \tag{17}$$

where $\mathcal{D}_+ u_- := \partial_t u_- + u_+ \cdot \nabla_x u_- + D_{qq}\Delta_x u_-$ is now the mean forward derivative of the backward velocity. We then sum up Eqs. (16) and (17) to get the following frictional version of the quantum Navier–Stokes equation (see for instance [21]):

$$\begin{aligned} \partial_t v + v \cdot \nabla_x v = & -\frac{1}{m}\nabla_x\big(V + \Lambda \log(n)\big) \\ & - D_{qq}^2 \left[ \big(\nabla_x \log(n) \cdot \nabla_x\big)\nabla_x \log(n) - \nabla_x \left( \frac{\Delta_x n}{n} \right) \right] , \end{aligned} \tag{18}$$

where $\Lambda$ is defined as in (7). Now it is clear that Eqs. (15) and (18) do constitute a closed system.

**Remark 1.** *Subtracting Eq.* (17) *from Eq.* (16) *yields*

$$(\partial_t + v \cdot \nabla_x)u_o - u_o \cdot \nabla_x v = (D_{qq}\Delta_x - 2\lambda)v - \frac{1}{n}\mathrm{div}_x(\mathbb{P}_{u_+}) ,$$

*or equivalently the following law for the stress tensor*

$$\mathrm{div}_x(\mathbb{P}_{u_+}) = 2D_{qq}\mathrm{div}_x\big(n\mathrm{Sym}(\nabla_x v)\big) - 2\lambda n v \tag{19}$$

*after having used the relations* (13)–(15)*, where we denoted*

$$\mathrm{Sym}(U) = \frac{1}{2}\big(U + U^T\big) ,$$

*given any tensor field $U$. It is then clear that* (19) *expresses now the closure relation required by Eqs.* (9) *and* (11) *in order that the hydrodynamic system associated with the WFPE becomes closed. As a matter of fact, Eq.* (18) *is nothing else than the quantum Navier–Stokes kernel with dissipative contribution (cf. Eq.* (15) *in* [21]*, which in this case would be just reduced to its classical version $\partial_t(nu) + \mathrm{div}_x(nu \otimes u) + \frac{1}{m}n\nabla_x V = 0$).*

**Remark 2.** *When initially dealing with the Caldeira–Leggett master equation, the same arguments as before can be applied to obtain the following equation for $v$*

$$\begin{aligned} \partial_t v + v \cdot \nabla_x v = & -\frac{1}{m}\nabla_x\big(V + \hbar\lambda\, \log(n)\big) \\ & - \frac{\hbar^2}{4m^2} \left[ \big(\nabla_x \log(n) \cdot \nabla_x\big)\nabla_x \log(n) - \nabla_x \left( \frac{\Delta_x n}{n} \right) \right] , \end{aligned}$$

*which incorporates standard quantum diffusion effects (with diffusion coefficient equal to $\frac{\hbar}{2m}$) at the hydrodynamic level.*

Returning now to the evolution governed by the (general) WFPE and combining Eqs. (12) and (18) with the relation (14), the equation for $u_+$ can be recovered

$$\begin{aligned} \partial_t u_+ + u_+ \cdot \nabla_x u_+ = & -\frac{1}{m}\nabla_x V - \frac{\Lambda}{m}\nabla_x \log(n) - \frac{2\alpha^2}{m\hbar^2}\nabla_x Q \\ & + D_{qq}\left[ \big(\nabla_x u_+ - \nabla_x u_+^T\big)\nabla_x \log(n) - \nabla_x(\nabla_x \cdot u_+) \right] , \end{aligned}$$

where $\alpha$ and $Q$ are defined as in the Introduction. Now, after identification of the velocity as an irrotational field, we get $u_+ = \frac{1}{m}\nabla_x S$, hence

$$\nabla_x\left(\partial_t S + \frac{1}{m}(\nabla_x S\cdot\nabla_x)\nabla_x S\right) = -\nabla_x\left(V + \frac{2\alpha^2}{\hbar^2}Q + \Lambda\,\log(n) + D_{qq}\Delta_x S\right),$$

which after integration with respect to $x$ yields the following Hamilton–Jacobi type equation for the evolution of $S$:

$$\partial_t S + \frac{1}{2m}\big|\nabla_x S\big|^2 = -V - \frac{2\alpha^2}{\hbar^2}Q - \Lambda\log(n) - D_{qq}\Delta_x S + \chi\,, \tag{20}$$

$\chi = \chi(t)$ being a function of time. Eq. (20) along with the continuity equation

$$\partial_t n + \frac{1}{m}\nabla_x\cdot(n\nabla_x S) = D_{qq}\Delta_x n \tag{21}$$

constitute a closed potential–flow quantum hydrodynamic system, so that an 'envelope' wavefunction may be constructed which contains the same physical information that the whole WFPE. To close this section, it is worthly to be noticed that under the original assumptions on the parameters we are straightforwardly led to $\alpha \ll \hbar$, which means that the quantum potential effects are drastically relaxed due to the spatial diffusion introduced by the WFPE. As consequence, the $D_{qq}$ term confers 'classical' behaviour to the system at the hydrodynamic level.

2.2. **The main dissipative model and its reduction to the purely logarithmic Schrödinger equation.** We consider the wavefunction

$$\Psi = \sqrt{n}\,e^{\frac{i}{\alpha}S}\,,\quad \alpha = 2mD_{qq}\,, \tag{22}$$

along with the quantization rule $m\oint_L \nabla_x S\,dl = 2k\pi$, where $k$ is an integer and $L$ is any closed loop, in order to keep $\Psi$ single–valued (see [36] and Theorem 3.3 in [20]). Then, we are led to the following Schrödinger–like equation accounting for frictional and dissipative effects

$$\begin{aligned} i\alpha\partial_t\Psi = {} & H_\alpha\Psi + \frac{\alpha^2}{\hbar^2}Q\Psi + \Lambda\log(n)\Psi \\ & + \alpha D_{qq}\left\{\frac{i}{2}\frac{\Delta_x n}{n} + \frac{m}{\hbar}\nabla_x\cdot\left(\frac{J_\Psi}{n}\right)\right\}\Psi\,, \end{aligned} \tag{23}$$

where $H_\alpha = -\frac{\alpha^2}{2m}\Delta_x + V$ is the electron Hamiltonian (under the new action unit $\alpha$, see the discussion at the end of this Section and [7] for details). In this picture, the probability density $|\Psi|^2$ coincides with $n$, while the current density $J_\Psi = \frac{\hbar}{m}\mathrm{Im}\big(\overline{\Psi}\nabla_x\Psi\big)$ is linked with $J$ by the relation $J_\Psi = \frac{\hbar}{\alpha}J$, $n$ and $J$ being as defined in (10). Notice that the function $\chi$ appearing in Eq. (20) has been set to zero in virtue of a simple change of global phase. Indeed, Eq. (23) is the (nonlinear) equation we postulate in the Schrödinger picture to model the

dissipative effects undergone by a quantum particle ensemble in contact with a thermal reservoir.

We recall that the $D_{pp}$–term, responsible for the decoherence process, does not contribute to the final form of Eq. (23). This is due to the fact that the moment system associated with the WFPE has been truncated at the level of the momentum equation, while the $D_{pp}$–contribution is only 'visible' at the next level, i.e. that of the energy equation. However, the role played by $D_{pp}$ is essential for the fulfillment of the uncertainty inequality as well as for the Lindblad form of the WFPE, thus for the positivity preservation of the density matrix operator. Indeed, a sufficient and necessary condition to fit the Kossakowski–Lindblad class is that the reservoir parameters be such that the inequality

$$D_{pp}D_{qq} - D_{pq}^2 \geq \frac{\hbar^2\lambda^2}{4}$$

holds (see [1] and references therein).

On the other hand, the position diffusion $D_{qq}$–term in the WFPE reveals as the more influential contribution to the structure of our model. First of all, it gives rise to a set of nonlinearities belonging to the so called Doebner–Goldin family [14], which is actually the most general class of nonlinear Schrödinger equations compatible with a Fokker–Planck continuity equation. Besides, we must notice that the diffusion governed by $D_{qq}$ turns the standard Schrödinger Hamiltonian $H$ into the effective one $H_\alpha$, where the presence of $\alpha$ instead of $\hbar$ contributes to mitigate the quantum effects exhibited by Eq. (23), as we already commented for Eq. (20).

Finally, we observe that the linear terms due to the $\lambda$–damping and the crossed (or 'anomalous') $D_{pq}$–diffusion in the WFPE are described in the wavefunction picture by a logarithmic nonlinearity (see (23) and the definition of $\Lambda$ in (7)). This kind of self–interaction, which can be seen as an expansion of $V$ up to $O(\hbar^2)$ when $V$ is assumed to be the Hartree electrostatic potential solving $\Delta_x V = n$ [17], becomes the most relevant contribution of Eq. (23). In fact, we can take advantage of the following nonlinear gauge transformation [31]

$$G\colon \Psi \longmapsto \Phi = \Psi \exp\left\{-\frac{i}{2}\log(n)\right\}, \tag{24}$$

which makes Eq. (23) equivalent to the (simpler) purely LSE

$$i\alpha\partial_t\Phi = H_\alpha\Phi + \Lambda\log(n)\Phi\,. \tag{25}$$

In this way, the Doebner–Goldin diffusive terms present in Eq. (23) might now be neglected only by turning the current density $J_\Psi$ into $J_\Phi = J_\Psi - \frac{\hbar}{2m}\nabla_x n$, which does not alter the observable velocity. $G$ is also revealed to enjoy sufficiently good properties (indeed, it preserves the local density and the Ehrenfest equations) so as to study various aspects of Eq. (23) via the LSE (25). This equation was introduced in [3] and mathematically analyzed in [5, 6, 19]. Also, a discussion about the physical meaning of the sign opposite to the logarithmic term can be

found in [8]. A variant of this equation was successfully derived in [23] to describe quantum Langevin processes and has been recently applied to the modeling of different phenomena such as magma transport or capillarity in fluids [11, 12, 24].

A rigorous proof of this equivalence has been recently developed in [20] under the more general framework established by the mapping

$$\mathcal{G}\colon \Psi \longmapsto \Phi = |\Psi| \, \exp\left\{ \frac{i}{\alpha}\Big( A\log(n) + BS \Big) \right\} ,$$

where $A$, $B$ are arbitrary real numbers and $S(t,x)$ is an argument function of $\Psi$. There, $\mathcal{G}$ is shown to be an homeomorphic transformation between both equations in a suitable functional space, thus preserving the dynamical behaviour.

Since we are mainly interested in the local densities associated with $\Psi$ and $\Phi$, which are identical to each other and also to that stemming from the Wigner function, we are called to focus further analysis on Eq. (23) and its gauge reduction to the purely LSE (25). Anyway, both Eqs. (23) and (25) retain the dissipative effects introduced by the WFPE.

The parameter $\alpha$ appearing in Eq. (23) has the dimensions of an action but it is not a universal constant, as it hinges on the particular system under study. Thus, though $\alpha \neq \hbar$ in general, it plays the role of $\hbar$ in some sense (see [7] for a wider discussion), confering quantum–mechanical meaning to our wavefunction. If we consider $\psi = \sqrt{n}\, e^{\frac{i}{\hbar}S}$ instead of $\Psi$ (cf. (22)), the continuity equation and Eq. (20) along with the quantization rule lead us to

$$\begin{aligned} i\hbar\partial_t\psi = H\psi + \left( \frac{2\alpha^2}{\hbar^2} - 1 \right) Q\psi + \Lambda \log(n)\psi \\ + D_{qq} \left\{ \frac{i\hbar}{2} \frac{\Delta_x n}{n} + m\nabla_x \cdot \left( \frac{J_\psi}{n} \right) \right\} \psi \, , \end{aligned} \tag{26}$$

that might be simplified into the so–called modular Schrödinger equation with coupling parameter $\kappa = 1 - \frac{\alpha^2}{\hbar^2}$ augmented by a logarithmic nonlinearity

$$i\alpha\partial_t\phi = H_\alpha\phi - \kappa Q\phi + \Lambda\log(n)\phi \, , \tag{27}$$

by making use of the gauge transformation

$$g\colon \psi \longmapsto \phi = \psi \, \exp\left\{ -\frac{i\alpha}{2\hbar} \, \log(n) \right\} .$$

For $\kappa = 1$, the modular equation does not admit exponentially confined solutions but can be derived from a local Lagrangian (see [2, 16]). Besides, its associated hydrodynamics does not contain quantum effects. As we have already observed, the effects derived from the action of the quantum potential in Eq. (20) are quite close to be negligible. The choice of $\psi$ and $\phi$ as envelope wavefunctions (instead of their counterparts $\Psi$ and $\Phi$) highlights this 'quantum relaxation' in Eq. (27) since $\kappa \simeq 1$. However, taking $\alpha$ as the action unit proves to be the most suitable choice because it makes the model simpler (avoiding the presence of $Q$ in Eq. (25)).

A final remark concerning the Caldeira–Leggett approach is now in order.

**Remark 3.** *In the particular case of the Caldeira–Leggett master equation (i.e. Eq.* (1)–(2) *with* $D_{pq} = D_{qq} = 0$*), our approach gives rise to the following potential–flow quantum hydrodynamic system*

$$\partial_t n = -\frac{1}{m}\nabla_x \cdot (n\nabla_x S) + \frac{\hbar}{2m}\Delta_x n\,,$$
$$\partial_t S = -\frac{1}{2m}|\nabla_x S|^2 - V - 2Q - \hbar\lambda\,\log(n) - \frac{\hbar}{2m}\Delta_x S + \chi\,.$$

*If we introduce the Madelung wavefunction* $\psi = \sqrt{n}\,e^{\frac{i}{\hbar}S}$*, its temporal evolution is shown to be ruled by the Schrödinger–like equation*

$$i\hbar\partial_t\psi = H\psi + Q\psi + \hbar\lambda\,\log(n)\psi + \frac{i\hbar^2}{4m}\frac{\Delta_x n}{n}\psi + \frac{\hbar}{2}\nabla_x\cdot\left(\frac{J_\psi}{n}\right)\psi\,, \tag{28}$$

*with* $H$ *standing for the usual electron Hamiltonian, which is analogous to that for the general case by taking* $\alpha = \hbar$*. In turn, this equation might be simplified to*

$$i\hbar\partial_t\phi = H\phi + \hbar\lambda\,\log(n)\phi\,,$$

*through the transformation* $\phi = \psi\exp\{-\frac{i}{2}\log(n)\}$*.*

## 3. Steady state dynamics

This section is devoted to explore the existence of solutions to Eq. (23) with constant local density, making special emphasis in the dynamics of radial solutions. Throughout this section, we consider a unit system for which $\hbar = m = k_B = 1$ for the sake of simplicity, and use the transformation given in (24) in order to investigate Eq. (25) instead of Eq. (23). Indeed, in this system of units Eq. (25) can be rewritten as

$$i\frac{\partial\Phi}{\partial t} = -\frac{\alpha}{2}\Delta_x\Phi + \frac{1}{\alpha}\big(V + \Lambda\log(n)\big)\Phi\,. \tag{29}$$

Notice that the definition of $G$ given in (24) straightforwardly leads to $|\Psi|^2 = |\Phi|^2$ (henceforth denoted by $n$), and

$$J_\Psi = J_\Phi + \frac{1}{2}\nabla_x n = \frac{1}{\alpha}J\,, \tag{30}$$

where $n$ and $J$ are the $\xi$–moments of the Wigner functions defined in (10).

We are intended to construct solutions of Eq. (23) that satisfy the stationary condition $\partial_t n = 0$, so that the divergence of the diffusion current $J - D_{qq}\nabla_x n$ must vanish in terms of the continuity equation (9). Specifically, we shall deal with the particular case in which $J = D_{qq}\nabla_x n$ (that is, the diffusion current is set to zero). In other words, we are considering the following current density distribution $J_\Psi = \frac{1}{2}\nabla_x n$ or, in the context of Eq. (29), $J_\Phi = 0$ (cf. formula (30)).

Of course, this situation obviously leads to stationary profiles $n(t,x) = n_0(x)$. In this setting, we search for solutions with the form

$$\Phi(t,x) = |\Phi_0(x)|\, e^{i\nu(t)}\,. \tag{31}$$

The necessary condition for such a solution to exist is

$$\nu' = \frac{\alpha}{2}\frac{\Delta_x|\Phi_0|}{|\Phi_0|} - \frac{1}{\alpha}\big(V + 2\Lambda\log(|\Phi_0|\big) = -\beta \in \mathbb{R}\,, \tag{32}$$

as follows from insertion of (31) into Eq. (29), which finally means that $\nu(t)$ is subject to linear growth, $\nu(t) = -\beta t + k$ with $k \in \mathbb{R}$. Therefore, the uniparametric family of wavefunctions $\Phi(t,x) = |\Phi_0(x)|\, e^{-i\beta t}$ are steady state solutions (up to a constant phase factor) of Eq. (25) with constant density. Now, by applying $G^{-1}$ we are led to the associated stationary profiles of Eq. (23) given by

$$\Psi(t,x) = |\Phi_0(x)|\exp\big\{i\big(\log(|\Phi_0(x)|) - \beta t\big)\big\}\,. \tag{33}$$

It is remarkable that for the free particle case ($V = 0$), Eq. (29) is Galilean invariant. Then, since the gauge transformation preserves this property (see for instance [31]), the Schrödinger equation for $\Psi = G^{-1}(\Phi)$ is Galilean invariant too. As a consequence, for any solution $\Psi$ and $v \in \mathbb{R}^N$, the wavefunctions given by

$$\Psi^v(t,x) := \Psi(t, x - vt)\exp\left\{-\frac{i}{\alpha}\left(\frac{1}{2}|v|^2 t - v\cdot x\right)\right\}$$

constitute a new family of solutions.

The rest of this section will be concerned with the finding of explicit solutions to Eq. (32) in different situations.

3.1. **Exponential profiles.** When searching for solutions as in (31) with exponential density profile $\Phi_0(x) = e^{A|x|^2+B}$ ($A, B \in \mathbb{R}$), we are led to the necessary condition

$$\Delta_x|\Phi_0| = \big(2NA + 4A^2|x|^2\big)\, e^{A|x|^2+B}\,,$$

so that Eq. (32) now reads

$$\beta\alpha + N\alpha^2 A - 2\Lambda B - V = 2A(\Lambda - \alpha^2 A)|x|^2\,.$$

In case that $V \equiv 0$ we obtain (up to a constant change of phase) $A = \frac{\Lambda}{\alpha^2}$ and $B = \frac{\beta\alpha}{2\Lambda} + \frac{N}{2}$, which leads to

$$\Phi(t,x) = \exp\{\gamma(|x|) - i\beta t\}\,, \quad \text{with } \gamma(r) = \frac{\Lambda}{\alpha^2}r^2 + \frac{\beta\alpha}{2\Lambda} + \frac{N}{2}\,.$$

Then, translated into the context of Eq. (23) we get

$$\Psi(t,x) = G^{-1}(\Phi)(t,x) = \exp\big\{\gamma(|x|) + i(\gamma(|x|) - \beta t)\big\}\,.$$

The plot on the left side in Figure 1 shows the modulus of some of these solutions under several coupling strengths for typical high temperature values of the coefficients $(T, \Omega, \lambda)$ within Dekker's phenomenology [10, 33]. One important feature to be stressed at this point is the absence of Gaussons due to the positive sign

of the coefficient preceeding the logarithmic term (see [8] for a discussion), that contrarily do exist if the opposite sign is chosen [5].

For the harmonic potencial $V(x) = \omega_0^2|x|^2/2$ we find

$$A_\pm = \frac{1}{2\alpha^2}\left(\Lambda \pm \sqrt{\Lambda^2 + \omega_0^2\alpha^2}\right) ,$$

that corresponds to

$$B_\pm = \frac{\beta\alpha}{2\Lambda} + \frac{N}{4\Lambda}\left(\Lambda \pm \sqrt{\Lambda^2 + \omega_0^2\alpha^2}\right) .$$

This straightforwardly yields

$$\Phi_\pm(t,x) = \exp\{\gamma_\pm(|x|) - i\beta t\} , \qquad \text{with} \;\; \gamma_\pm(r) = A_\pm r^2 + B_\pm .$$

Translated again into the context of Eq. (23), we finally get two biparametric families of solutions given by

$$\Psi_\pm(t,x) = G^{-1}(\Phi)(t,x) = \exp\big\{\gamma_\pm(|x|) + i(\gamma_\pm(|x|) - \beta t)\big\} .$$

Notice that in this case $\Psi_-$ is a Gausson of Eq. (29). Several examples of such profiles are represented in the plot on the right–hand side in Figure 1.

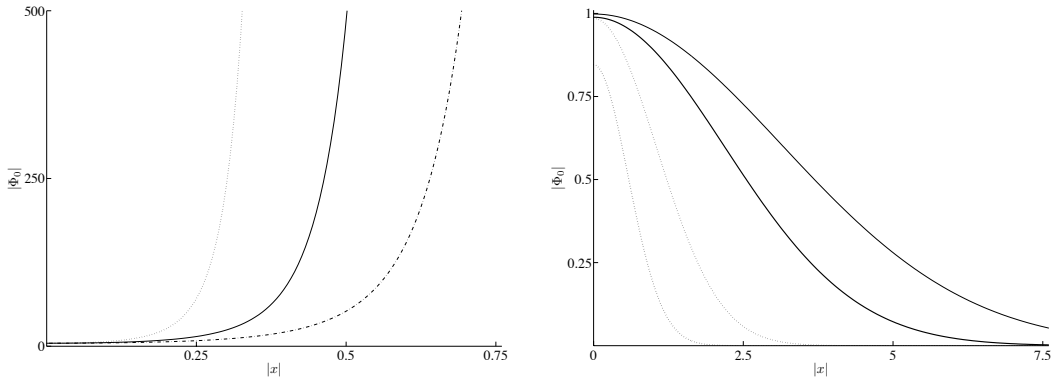


FIGURE 1. Radial solutions with exponential shape of Eq. (32) for $N = 3$, $\beta = 0$ (ground states) and $T = 2$, $\Omega = 1$. From left to right: (i) $V = 0$ with increasing switching of the coupling parameter: $\lambda = 0.05$ (dashed line), $\lambda = 0.15$ (continuous) and $\lambda = 0.5$ (dashed–pointed line). (ii) The harmonic potential $V(x) = \omega_0^2|x|^2/2$ with $\lambda = 0.05$ and frequencies $\omega_0 = 0.075$ (thin–dashed line) and $\omega_0 = 0.025$ (thin–continuous line); and with $\lambda = 0.25$ and frequencies $\omega_0 = 0.4$ (thick–dashed line) and $\omega_0 = 0.1$ (thick–continuous line), respectively.

3.2. **Solutions depending upon** $s(x) = \sum_{j=1}^{N} x_j$**.** It also proves of interest to find nontrivial solutions of Eq. (32) as functions of the symmetric polynomial $s(x) = x_1 + x_2 + \cdots + x_N$ in the free–particle case (indeed, it is remarkable the fact that for the harmonic potencial case, it is not possible to write down an equation only depending upon $s$). As a matter of fact, in considering the position density ansatz $|\Phi_0(x)| = y(s(x))$ we can deduce

$$\beta = -\frac{N\alpha}{2}\frac{y''}{y} + \frac{2\Lambda}{\alpha}\log(y)\,. \tag{34}$$

Now, taking $y(s) = \exp\{Cs^a + D\}$ we are necessarily led (up to a constant change of phase) to

$$a = 2\,, \quad C = \frac{\Lambda}{N\alpha^2}\,, \quad D = \frac{1}{2} + \frac{\beta\alpha}{2\Lambda}\,,$$

that gives

$$\Phi(t,x) = \exp\left\{\gamma\big(s(x)/\sqrt{N}\big) - i\beta t - \frac{N-1}{2}\right\}\,.$$

Hence, the wavefunction profiles

$$\Psi(t,x) = \exp\left\{\gamma\big(s(x)/\sqrt{N}\big) - \frac{N-1}{2} + i\left(\gamma(s(x)/\sqrt{N}) - \frac{N-1}{2} - \beta t\right)\right\}$$

satisfy Eq. (23). To find a relation between $y$ and $y'$ we are just called to multiply the identity (34) by $yy'$ and integrate against $s$ to get

$$(y')^2 - \frac{2\beta}{N\alpha}y^2 - \frac{2\Lambda}{N\alpha^2}y^2\big(\log(y^2) - 1\big) \equiv K_0 \in \mathbb{R}\,, \tag{35}$$

for which the only admissible saddle point is $\big(\exp\big\{-\beta\alpha/2\Lambda\big\}, 0\big)$. In order to remove the parameter $\beta$ we may introduce the scaling $y = y_0 Y$, where

$$y_0 = \exp\left\{\frac{1}{2} + \frac{\beta\alpha}{2\Lambda}\right\}$$

is the constant solution of Eq. (51) with $K_0 = 0$. This gives rise to the simpler equation

$$(Y')^2 - \frac{2\Lambda}{N\alpha^2}Y^2\log(Y^2) = \widetilde{K_0} \in \mathbb{R}\,, \tag{36}$$

that now has the saddle point at $\big(\exp\{-1/2\}, 0\big)$. Figure 2 below establishes a comparison among the phase portraits of this equation and those of the logarithmic equation proposed in [3] (with focusing nonlinearity).

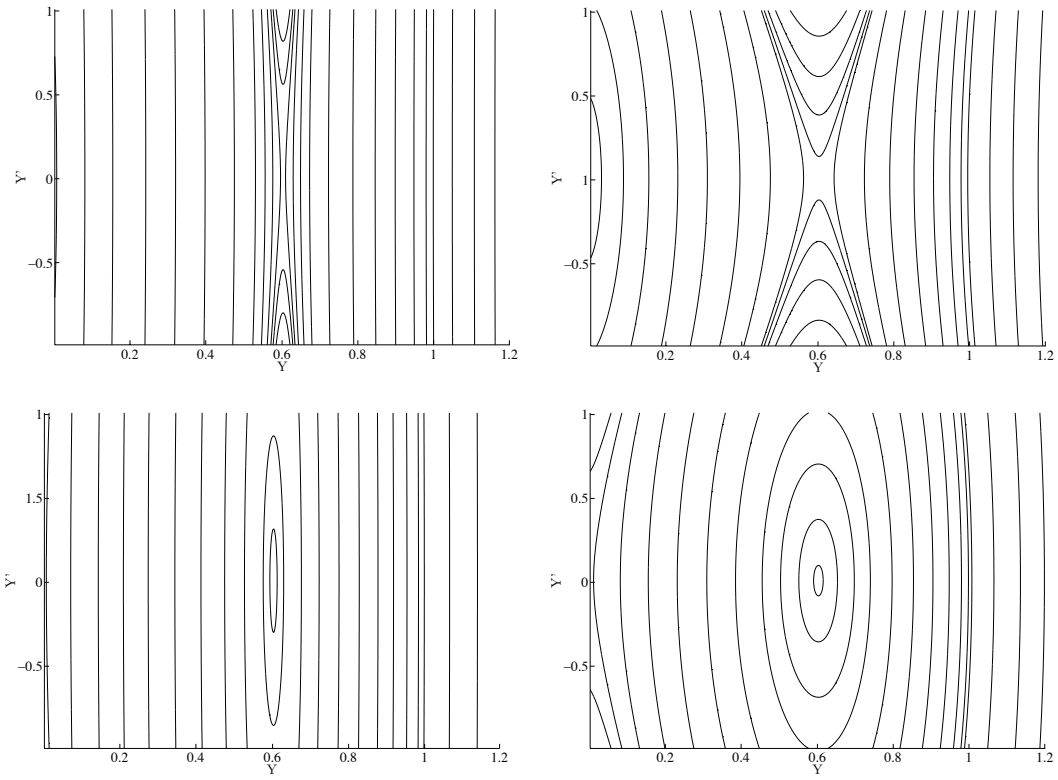


FIGURE 2. Left to right and top to bottom: The first two pictures show the phase portrait of Eq. (36) (with $\widetilde{K_0} = 0$) in three dimensions for the values of the parameters $T = 2$, $\Omega = 1$, and $\lambda = 0.01$ and $\lambda = 0.5$, respectively. The last two pictures correspond to the opposite sign for the logarithmic term.



3.3. **Radial solutions.** We finally investigate the radial (rotationally symmetric) solutions of Eq. (32). To this aim, consider $|\Phi_0(x)| = \varphi(r)$ with $r = |x|$. Then, $\Delta_x|\Phi_0| = \frac{N-1}{r}\varphi' + \varphi''$ and Eq. (32) does become

$$\beta = -\frac{\alpha}{2}\left(\frac{N-1}{r}\frac{\varphi'}{\varphi} + \frac{\varphi''}{\varphi}\right) + \frac{1}{\alpha}V + \frac{\Lambda}{\alpha}\log(\varphi)\,.$$

Using the change of variables $\varphi = \exp\{\beta\alpha/(2\Lambda)\}z$ we find the following ($\beta$–independent) equation for the density profile $z$:

$$z'' - \frac{(z')^2}{2z} + (N-1)\frac{z'}{r} - \frac{4}{\alpha^2}Vz - \frac{2\Lambda}{\alpha^2}\log(z^2)z = 0\,, \tag{37}$$

Eq. (37) can be solved numerically using the classical Runge–Kutta scheme with $z'(0) = 0$ in order to avoid the singularity at the origin. As a result, we obtain compactly supported density profiles $\Phi_0$ to Eq. (32) for both potentials $V = 0$

and $V(x) = \frac{1}{2}\omega_0^2|x|^2$ (see Figure 3 for some examples). As consequence, Eq. (23) also admits rotationally symmetric, compactly supported steady states.

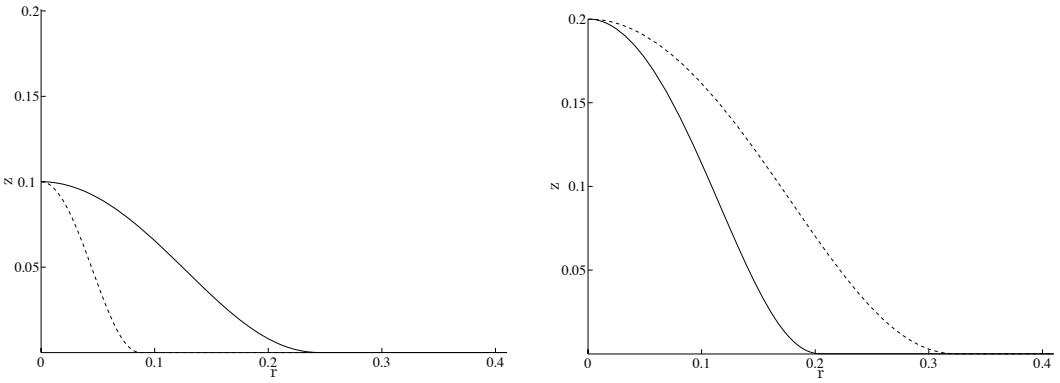


FIGURE 3. Numerical solutions of Eq. (37) in three dimensions for $T = 2$, $\Omega = 1$. From left to right: (i) $V = 0$ with initial data $z(0) = 0.1$, $z'(0) = 0$ and the following values of the coupling coefficient: $\lambda = 0.1$ (continuous line) and $\lambda = 0.01$ (dashed line). (ii) $V(x) = \frac{1}{2}\omega_0^2|x|^2$ with initial data $z(0) = 0.2$, $z'(0) = 0$ and the following values of the pair frequency–coupling parameter: $\omega_0 = 0.05$ and $\lambda = 0.15$ in the overdamped case (dashed line), $\omega_0 = 0.3$ and $\lambda = 0.05$ in the underdamped case (continuous line). Numerically, these profiles are observed to be unstable when changing the initial data.

## 4. Numerical comparison of transient dynamics for the logarithmic Schrödinger and the Wigner–Fokker–Planck equations

The purpose of this section is to construct numerical solutions of the one dimensional version of Eq. (25) (that is recalled to be gauge equivalent to Eq. (23) according to the transformation introduced in (24)) and compare them to the exact solutions stemming from the corresponding WFPE. To this aim, we are intended to extend the discretization procedure introduced in [34] in the setting of Schrödinger–Poisson models to our context (cf. Appendix B). We will particularly focus our attention on the macroscopic information shed by the position standard deviation $\sigma_X$ (see formula (39) below), which constitutes an accurate measure of the (statistically) dispersive behaviour peculiar to these equations.

4.1. **Theoretical framework.** This paragraph is devoted to set up the main differential laws that determine the time evolution of $\sigma_X$ from both the Wigner–Fokker–Planck and the logarithmic Schrödinger pictures. Since the LSE is written in a much smaller scale than that of the WFPE (we recall on this point that $\alpha \ll \hbar$), we shall perform the numerical comparison using dimensionless equations based on adequate units of space, time and velocity (see Appendix A).

4.1.1. *The Wigner–Fokker–Planck setting.* We consider the dimensionless WFPE in 1D

$$w_t + \xi w_x + [V^\star]\theta_V(w) = [D_{pp}]w_{\xi\xi} + (\xi w)_\xi + [D_{pq}]w_{\xi x} + \frac{1}{2}w_{xx}\,, \tag{38}$$

in which formulation we have kept the notation $(t,\ x,\ \xi)$ for the kinetic variables, $w$ for the Wigner function, and $\theta$ for the pseudo–differential operator (cf. Eq. (48)), and where $[D_{pp}]$ and $[D_{pq}]$ are dimensionless constants (see Eq. (49) in Appendix A). Also, here and henceforth the subscripts $x$ and $t$ will denote the variables with respect to which differentiation is performed. We start by establishing the main notational conventions to be employed from here on. In this spirit, the particle and current densities $n$ and $J$ are those defined in (10), while the magnitudes

$$\big(P, \langle v\rangle, E, \langle x\rangle, \langle x^2\rangle\big)(t) = \int_{-\infty}^{\infty} \big(n, J, e, xn, x^2 n\big)(t,x)\,dx$$

represent (from left to right) the total probability and the expected values of the mean velocity, the kinetic energy, the position operator, and the square position operator associated with the Wigner function $w(t,x,\xi)$, respectively. Here, the kinetic energy density reads as

$$e(t,x) = \frac{1}{2}\int_{-\infty}^{\infty} \xi^2 w(t,x,\xi)\,d\xi\,.$$

The standard deviation from the mean position is then given by

$$\sigma_X = \sqrt{\langle x^2\rangle - \langle x\rangle^2}\,. \tag{39}$$

Below we shall analyze the time evolution of these quantities for the general case of an arbitrary real–valued potential $V = V(t,x)$, making especial emphasys on the free particle and the harmonic oscillator models. Also, the notation $E_0 = E(0)$, $\langle x^k\rangle_0 = \langle x^k\rangle(0)$ and $\langle v\rangle_0 = \langle v\rangle(0)$ will be adopted for the powers $k = 1, 2$, as well as an analogous notation for their corresponding derivatives.

Concerning Eq. (38), the more relevant information for our purpose is contained in the following

**Lemma 1.** *Let $V = V(t,x)$ be any real–valued potential and $w$ a smooth solution of the Wigner–Fokker–Planck equation (38). Then, the following identities hold true:*

(i) $\langle x\rangle'' + \langle x\rangle' = -F_V$.
(ii) $\langle x^2\rangle'' + \langle x^2\rangle' = -2G_V + 4E + 2[D_{pq}] + 1$.
(iii) $E' + 2E = -H_V + [D_{pp}]$.

*Here, we denoted*

$$F_V = [V^\star]\int_{-\infty}^{\infty} nV_x\,dx\,, \quad G_V = [V^\star]\int_{-\infty}^{\infty} xnV_x\,dx\,, \quad H_V = [V^\star]\int_{-\infty}^{\infty} JV_x\,dx\,,$$

*whereas* $[V^\star]$ *is given in* (49). *In addition, the total probability is preserved along the time evolution, that is,* $P(t) \equiv 1$ *(after appropriate normalization). Furthermore, the following relation is also fulfilled:*

(iv) $\langle x^2\rangle'(t) = 2\displaystyle\int_{-\infty}^{\infty} xJ\,dx + 1.$

**Proof.** The hydrodynamic system associated with Eq. (38), up to first order $\xi$–moments, is easily shown to be given by

$$n_t + J_x = \frac{1}{2} n_{xx}\,, \tag{40}$$

$$J_t + 2e_x + [V^\star] n V_x = -J - [D_{pq}] n_x + \frac{1}{2} J_{xx}\,, \tag{41}$$

$$e_t + \frac{1}{2}\int_{-\infty}^{\infty} \xi^3\, w_x\, d\xi + [V^\star] J V_x = [D_{pp}] n - 2e - [D_{pq}] J_x + \frac{1}{2} e_{xx}\,, \tag{42}$$

after multiplying (formally) Eq. (38) by $\xi^k$ and integrating against $\xi$ for $k = 0, 1, 2$, respectively.

On one hand, we observe that (i) follows straightforwardly from Eqs. (40) and (41). On the other hand, multiplying Eq. (40) times $x^2$ and integrating with respect to $x$ leads to

$$\langle x^2\rangle'(t) = 2\int_{-\infty}^{\infty} xJ\,dx + P(t)\,.$$

Since integration of Eq. (40) entails that $P(t)$ is time preserved, we can normalize it to unity to get (iv). Furthermore, differentiating (iv) with respect to time and using Eq. (41) yield (ii). Finally, multiplication of Eq. (38) times $\frac{1}{2}\xi^2$ and subsequent integration against $x$ and $\xi$ imply (iii). □

Notice that the ODEs appearing in Lemma 1 allow us to address the study of the Wigner–Fokker–Planck transient dynamics without an explicit knowledge of the Wigner function. Indeed, for our distinguished examples the setting is as follows.

(i) In the free particle case ($V = 0$), it is clear that $F_V = G_V = H_V = 0$. Then, the equations established in Lemma 1 (i)–(iii) can be solved explicitely to give the following expressions for $\langle x\rangle$ and $\langle x^2\rangle$:

$$\langle x\rangle(t) = \langle x\rangle_0 + \langle v\rangle_0\big(1 - e^{-t}\big)\,,$$

$$\langle x^2\rangle(t) = \langle x^2\rangle_0 + At + \big(\langle x^2\rangle_0' - A\big)\big(1 - e^{-t}\big) + \frac{B}{2}\big(1 - e^{-t}\big)^2, \tag{43}$$

where we denoted

$$A = 2[D_{pp}] + 2[D_{pq}] + 1\,, \quad B = 4E_0 - 2[D_{pp}]\,.$$

(ii) In the harmonic oscillator case, the pseudo–differential term in Eq. (38) can be proved to read $[V^\star]\theta_V(w) = -\big(\frac{\omega_0}{2\lambda}\big)^2 x w_\xi$. Hence, we have

$$F_V = \Big(\frac{\omega_0}{2\lambda}\Big)^2 \langle x\rangle\,, \quad G_V = \Big(\frac{\omega_0}{2\lambda}\Big)^2 \langle x^2\rangle\,, \quad H_V = \frac{\omega_0^2}{8\lambda^2}\big(\langle x^2\rangle'(t) - 1\big)\,,$$

so that all of the equations in Lemma 1 are realized to depend upon the strength of the damping. Indeed, we have

$$\langle x\rangle_{\text{over,under}}(t) = e^{-\frac{t}{2}}\, X_{\text{over,under}}(t)\,,$$

where $X_{\text{over}}(t)$ reads

$$\langle x\rangle_0\, \cosh\Big(\frac{1}{2\lambda}\sqrt{\lambda^2 - \omega_0^2}\; t\Big) + \frac{\lambda\big(\langle x\rangle_0 + 2\langle v\rangle_0\big)}{\sqrt{\lambda^2 - \omega_0^2}}\, \sinh\Big(\frac{1}{2\lambda}\sqrt{\lambda^2 - \omega_0^2}\; t\;\Big)\,,$$

while $X_{\text{under}}(t)$ is given by

$$\langle x\rangle_0\, \cos\Big(\frac{1}{2\lambda}\sqrt{\omega_0^2 - \lambda^2}\; t\Big) + \frac{\lambda\big(\langle x\rangle_0 + 2\langle v\rangle_0\big)}{\sqrt{\omega_0^2 - \lambda^2}}\, \sin\Big(\frac{1}{2\lambda}\sqrt{\omega_0^2 - \lambda^2}\; t\;\Big)\,,$$

for the overdamped ($\lambda > \omega_0$) and the underdamped ($\lambda < \omega_0$) regimes, respectively, as follows from straightforward calculations. Observe that brackets notation can be skipped here, as explained in Appendix A (cf. (51)). As well, the system (ii)–(iii) governing the evolution of $\langle x^2\rangle$ will be solved by means of the classical Runge–Kutta method, in order to compute $\sigma_X$ (see Figures 6 and 7 below).

4.1.2. *The Schrödinger setting.* The gauge–reduced LSE we deal with in this section reads as follows

$$i\Phi_t = -\frac{1}{2}\Phi_{xx} + \big([V^\star]V + [\Lambda]\log(n_\Phi)\big)\Phi\,, \tag{44}$$

where $[\Lambda] = \frac{1}{2} + [D_{pq}]$. In this picture, the particle and current densities are respectively defined by

$$n_\Phi = |\Phi|^2\,, \quad J_\Phi = \mathrm{Im}\big(\overline{\Phi}\Phi_x\big)\,,$$

whereas the magnitudes

$$\big(P_\Phi, \langle v\rangle_\Phi, \langle x\rangle_\Phi, \langle x^2\rangle_\Phi\big)(t) = \int_{-\infty}^{\infty} \big(n_\Phi, J_\Phi, x n_\Phi, x^2 n_\Phi\big)(t,x)\, dx$$

have the same meaning that their counterparts defined in the previous section. The expected kinetic energy is now given by

$$E_\Phi(t) = \frac{1}{2}\int_{-\infty}^{\infty} |\Phi_x(t,x)|^2\, dx\,. \tag{45}$$

The standard deviation from the mean position is defined as in (39), by just considering $\langle x^k\rangle_\Phi$ instead of $\langle x^k\rangle$, for $k = 1, 2$.

We shall carry over the calculations for an arbitrary potential, in order to fit the examples of our interest later on in the numerical simulations presented in this paper. The relevant evolution laws for our purposes are collected in the following

**Lemma 2.** *Let $V = V(t,x)$ be any real–valued potential and $\Phi$ a smooth solution of the LSE (44). Then, the following identities hold true:*

(i) $\langle x\rangle''_\Phi = -F_V^\Phi$.

(ii) $\langle x^2\rangle''_\Phi = -2G_V^\Phi + 4E_\Phi + 2[D_{pq}] + 1$.

(iii) $E'_\Phi + \Big([D_{pq}] + \dfrac{1}{2}\Big)\displaystyle\int_{-\infty}^{\infty} \log(n_\Phi)_x J_\Phi\, dx = -H_V^\Phi$,

*where the integrals $F_V^\Phi$, $G_V^\Phi$ and $H_V^\Phi$ are defined as in Lemma 1 with $n_\Phi$ and $J_\Phi$ instead of $n$ and $J$. In addition, the total probability is preserved along the time evolution, that is, $P_\Phi(t) \equiv 1$ (after appropriate normalization), and the following relation is also fulfilled:*

(iv) $\langle x^2\rangle'_\Phi = 2\displaystyle\int_{-\infty}^{\infty} xJ_\Phi\, dx$.

**Proof.** We first observe that the preservation of $P_\Phi$ as well as the identity $\langle x\rangle'_\Phi = \langle v\rangle_\Phi$ follow immediately from differentiating the expression for $\langle x\rangle_\Phi$ and employing Eq. (44) properly. Also, differentiation of $\langle v\rangle_\Phi$ yields

$$\langle v\rangle'_\Phi = \mathrm{Im}\int_\infty^\infty \big\{\overline{\Phi}_t\Phi_x + \overline{\Phi}\Phi_{tx}\big\}\, dx\,.$$

In order to calculate this integral we use again Eq. (44) and the real–valuedness of $V$ to conclude that

$$\langle v\rangle'_\Phi = -[V^\star]\int_\infty^\infty n_\Phi V_x\, dx\,,$$

which implies (i). On the other hand, (iv) easily follows from differentiating $\langle x^2\rangle_\Phi$. Besides, the second derivative of this quantity can be computed as

$$\langle x^2\rangle''_\Phi = 2\mathrm{Im}\int_\infty^\infty x\big\{\overline{\Phi}_t\Phi_x + \overline{\Phi}\Phi_{tx}\big\}\, dx\,.$$

Now, performing the same calculations as before and identifying terms, we obtain (ii). Finally, (iii) arises from differentiation of $E_\Phi$, use of Eq. (44), and convenient integration by parts. □

In the free particle case, Lemma 2 (i) informs that the expected position evolves linearly in time according to $\langle x\rangle_\Phi(t) = \langle x\rangle_{\Phi,0} + \langle v\rangle_{\Phi,0}\, t$, while for the case of the harmonic oscillator one has

$$\langle x\rangle_\Phi(t) = \langle x\rangle_{\Phi,0}\cos\Big(\frac{\omega_0}{2\lambda}t\Big) + \frac{2\lambda\langle v\rangle_{\Phi,0}}{\omega_0}\sin\Big(\frac{\omega_0}{2\lambda}t\Big)\,.$$

Note that we are using again the relation $\frac{[\omega_0]}{[\lambda]} = \frac{\omega_0}{\lambda}$ to avoid unnecessary brackets. It is also obvious that the system (ii)–(iii) in Lemma 2 is not self–consistent for the determination of $\langle x^2 \rangle$. Indeed, even if $V$ is set to zero (which is the simplest case we investigate here), Eq. (iii) in Lemma 2 leads to

$$E'_\Phi(t) = -\left([D_{pq}] + \frac{1}{2}\right) \int_{-\infty}^{\infty} \log(n_\Phi)_x J_\Phi \, dx \,,$$

so that (ii)–(iii) does not fit the form of a closed system. As consequence, all of the calculations concerning observable quantities for the LSE are to be performed from the perspective of a numerical approach, in the spirit of the scheme developed in Appendix B.

When comparing the evolution laws proven in Lemmata 1 and 2, it can be immediately observed that the only structural difference affecting the equations for $\langle x \rangle$ and $\langle x^2 \rangle$ lies in the absence of the $\lambda$–damping terms at the Schrödinger level. Of course, this entails by no means that these effects are lost via our derivation. At variance, friction effects are still present in Eqs. (ii) and (iii) of Lemma 2, mainly through the integral term in (iii) which involves a combination of the interaction parameters stemming from the original WFPE. The behaviour of $\sigma_X$ will then reveal mainly influenced by the damping terms affected by $[D_{pq}]$ and $[\lambda]$, which are the two more relevant contributions in our models as commented in § 2.2.

4.2. **Simulations.** This section is devoted to the presentation of the one–dimensional numerical simulations for the positional dispersion (quantified through the standard deviation $\sigma_X$) of the solutions to Eq. (44) as compared with that associated with the exact solutions of Eq. (38).

To this aim, the choice of the physical parameters $[\lambda]$, $[\Omega]$, $[\omega_0]$, and $[T]$ has been subject to the fulfillment of the assumptions (H1)–(H3) stated in the Introduction. Indeed, in the Figures below we have kept $[T] = 0.8$ and $[\Omega] = 1$ fixed, while varied $[\lambda] = 0.25, 0.3, 0.35, 0.4$. Also, when dealing with the harmonic oscillator we have used $[\omega_0] = 0.1\pi$. We call the reader to realize that $\sigma_X$ is expressed in length units referred to $L^\star$ (see Appendix A for a comprehensive statement of the meaning of $\star$–superscripts and parameters between brackets).

As initial data we choose single Gaussian profiles with mean position $x_0$ and mean velocity $\xi_0$, namely

$$w_0(x,\xi) = \left(2\pi\sigma_{X,0}\sigma_{V,0}\right)^{-1} \exp\left\{-\frac{(x-x_0)^2}{2\sigma_{X,0}^2} - \frac{(\xi-\xi_0)^2}{2\sigma_{V,0}^2}\right\} \,,$$

$\sigma_{X,0}$ and $\sigma_{V,0}$ denoting the initial standard deviations for the position and the velocity, respectively. Note that the election of $\sigma_{X,0}$ and $\sigma_{V,0}$ is constrained by

Heisenberg's uncertainty principle, which in our unit system reads

$$\sigma_{X,0}\sigma_{V,0} \geq \frac{\hbar}{2\alpha} = 1.9335\frac{[T]}{[\lambda]}\,. \tag{46}$$

In the sequel, $\sigma_{V,0}$ will be chosen to fulfill the equality in (46). Translated into the wavefunction picture, these initial data correspond to

$$\Phi_0(x) = \left(2\pi\sigma_{X,0}^2\right)^{-\frac{1}{4}} \exp\left\{-\frac{(x-x_0)^2}{4\sigma_{X,0}^2} + i\left(\xi_0 x + \frac{(x-x_0)^2}{4\sigma_{X,0}^2}\right)\right\}\,,$$

as can be checked by performing to a large extent the same construction carried out along Section 2, that is: Calculating the densities $n_0$ and $J_0$ associated with $w_0$ (as in Eq. (10)), extracting a scalar potential $S_0$ of $\frac{J_0}{n_0}$ (which is not necessarily unique), constructing the wavefunction $\Psi_0 = \sqrt{n_0}\, e^{iS_0}$, and lastly observing that $\Phi_0 = G(\Psi_0)$, where $G$ is the gauge transformation introduced in (24). Notice that $w_0$ and $\Phi_0$ are both normalized in such a way that the integrals of their probability densities amount one.

Associated with these profiles, there are the following initial values to be taken into consideration in the subsequent numerical solutions of Eqs. (ii) and (iii) in Lemma 1:

$$\langle x^2\rangle_0 = x_0^2 + \sigma_{X,0}^2\,, \quad \langle x^2\rangle_0' = 2x_0\xi_0 + 1\,, \quad E_0 = \frac{\xi_0^2}{2} + \frac{\sigma_{V,0}^2}{2}\,.$$

Regarding the numerical approximation of solutions to Eq. (44), the time step $dt$ has been chosen equal to $10^{-4}$ whereas the spatial mesh consists of the interval $[-35, 35]$ split into $10^4$ subintervals (that is, we selected the length interval $dx = 0.007$). We also stress that our simulations have been performed in the time interval $[0, 1]$, as in our dimensionless equations the (momentum) relaxation time has been set to unity. Figures 4 to 7 below plot the results shed by these simulations.

On one hand, Figures 4 and 5 show the time evolution of the standard deviation associated with numerical solutions to the (purely) LSE (44) and exact solutions to the Wigner–Fokker–Planck equation (38) calculated from Eq. (43), for the initial profiles introduced above and in the free particle case. In particular, these plots show how the fitness of both curves is modified according to the different variables taking part in the model. The action of the Fokker–Planck mechanism is indeed shown to be 'milder' in Eq. (44) than in Eq. (38), in the sense that the statistical dispersion of solutions to Eq. (44) is less changeable than that of solutions to Eq. (38) against increasing bias of the coupling parameter. Besides, the approximation is observed to improve as $[\lambda]$ grows.

On the other hand, Figures 6 and 7 still depict the time behaviour of the standard deviations of transient solutions to the LSE and the WFPE, now subject to the action of the harmonic oscillator potential. Here, the value of $\sigma_X$ associated with the Wigner function is computed numerically by solving system (ii)–(iii) in

Lemma 1. Unlike the previous case, it is now observed that the standard deviation associated with Eq. (38) is less changeable than that of Eq. (44) when increasing the strength of the coupling. Nevertheless, the conclusion is exactly the same as before: Larger values of $[\lambda]$ lead to better approximations of the Wigner function by the wavefunction. Finally we stress that, contrary to what one might expect, the oscillatory behaviour inherent to the harmonic potential is not manifested in our plots due to the restrictions on the physical parameters that make us to consider too low oscillation frequencies $[\omega_0]$, so that the period is necessarily much longer than the relaxation time in our parameter regime.

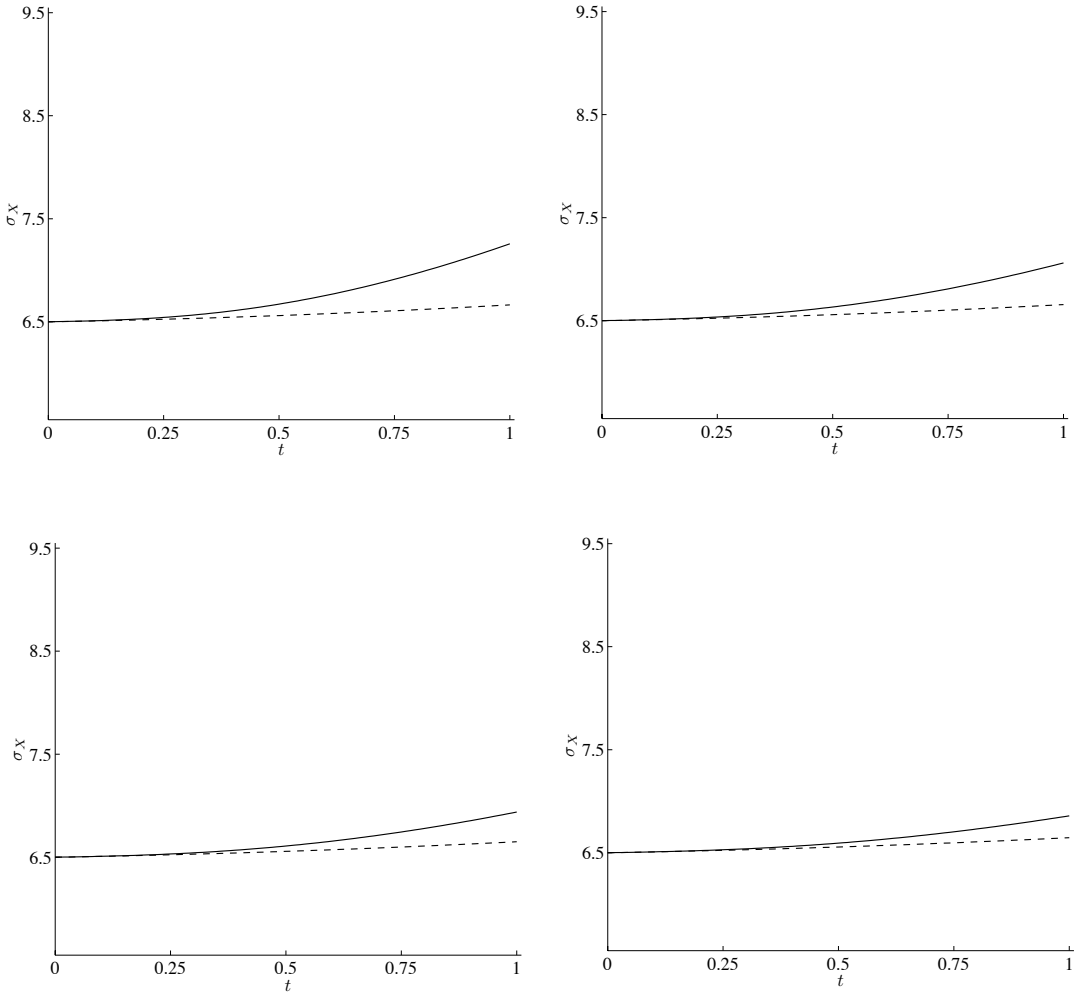


FIGURE 4. Evolution of the standard deviation of the exact solutions to Eq. (38) (continuous line) computed from Eq. (43), and of the numerical solutions of Eq. (44) (dashed line) in the free particle case, with $x_0 = \xi_0 = 0$, $\sigma_{X,0} = 6.5$, and increasing coupling (from left to right and top to bottom): $[\lambda] = 0.25, 0.3, 0.35, 0.4$.

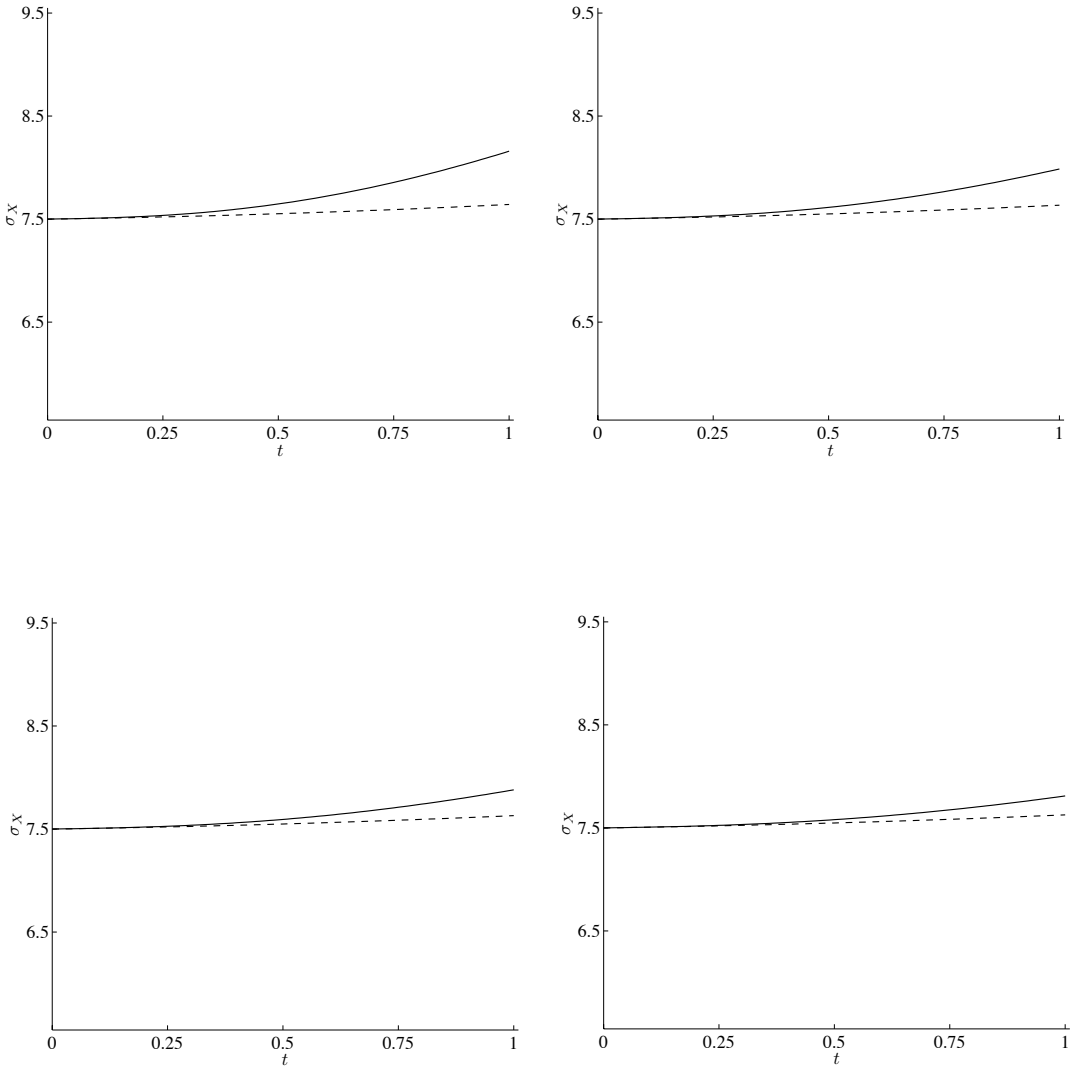


FIGURE 5. Evolution of the standard deviation of the exact solutions to Eq. (38) (continuous line) computed from Eq. (43), and of the numerical solutions of Eq. (44) (dashed line) in the free particle case, with $x_0 = \xi_0 = 0$, $\sigma_{X,0} = 7.5$, and increasing coupling (from left to right and top to bottom): $[\lambda] = 0.25, 0.3, 0.35, 0.4$.

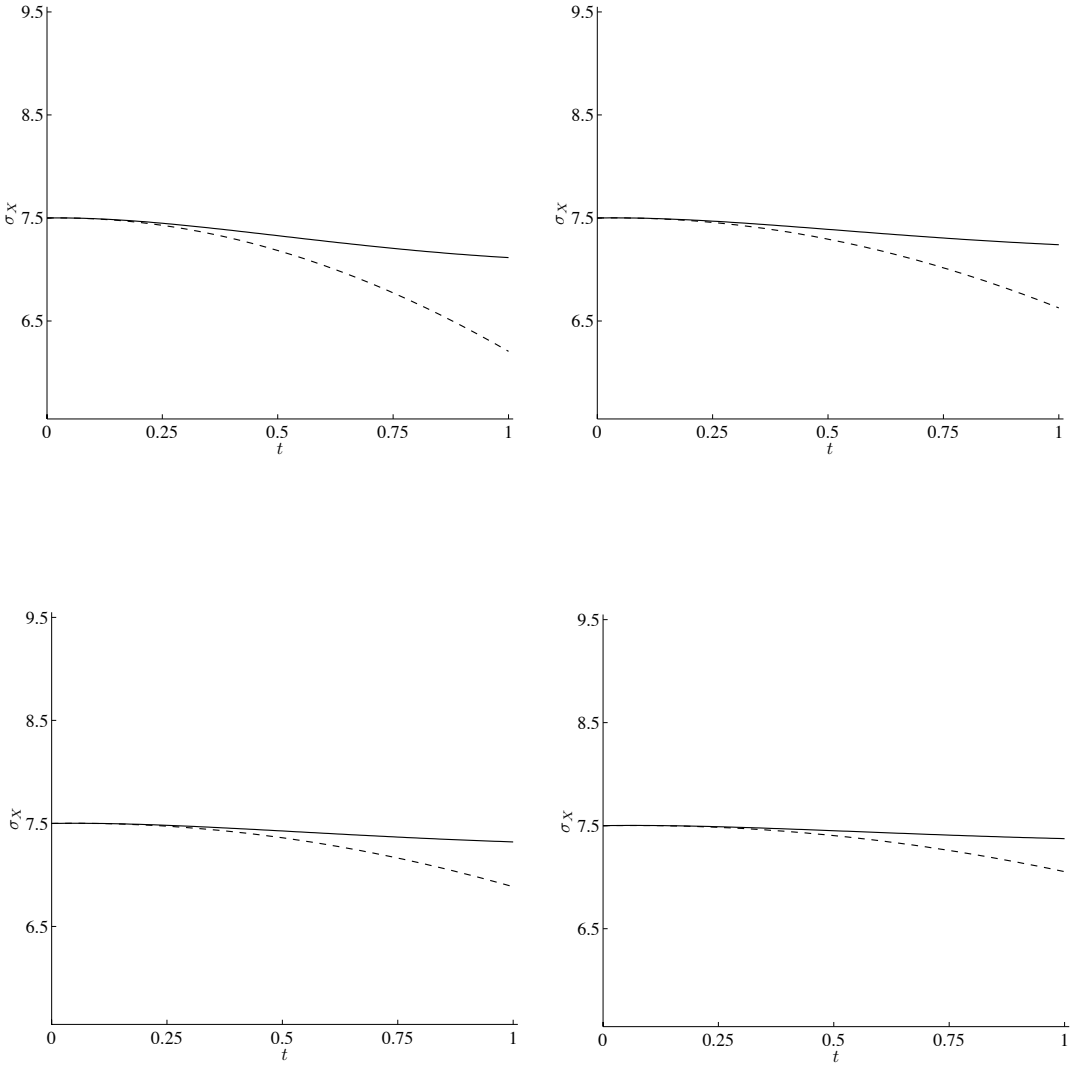


FIGURE 6. Evolution of $\sigma_X$ computed through system (ii)–(iii) in Lemma 1 (continuous line) and through the numerical solutions of Eq. (44) (dashed line) in the harmonic oscillator case, with $x_0 = 1$, $\xi_0 = 0$, $\sigma_{X,0} = 7.5$, angular frequency $[\omega_0] = 0.1\pi$, and increasing coupling (from left to right and top to bottom): $[\lambda] = 0.25, 0.3, 0.5, 0.4$.

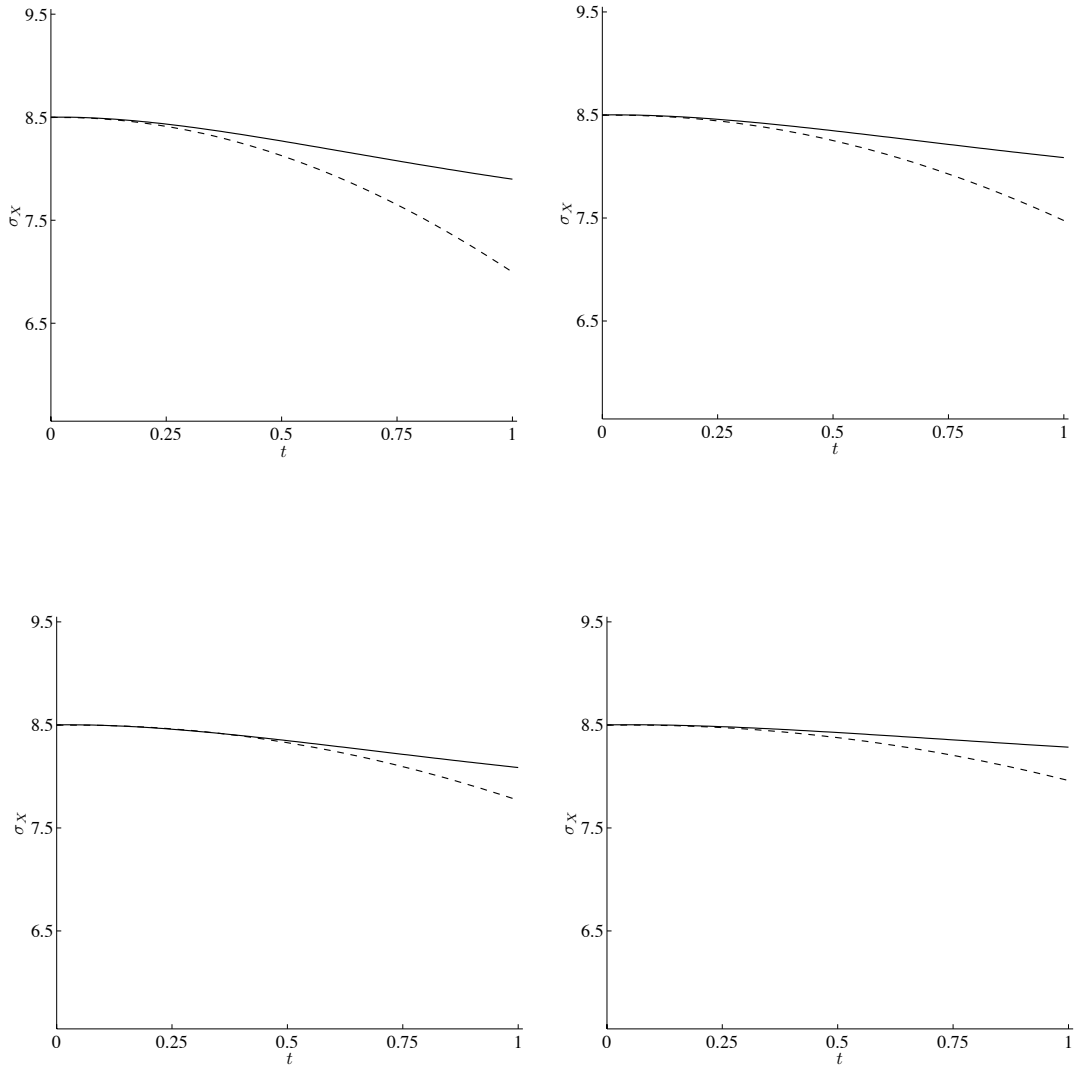


FIGURE 7. Evolution of $\sigma_X$ computed through system (ii)–(iii) in Lemma 1 (continuous line) and through the numerical solutions of Eq. (44) (dashed line) in the harmonic oscillator case, with $x_0 = 1$, $\xi_0 = 0$, $\sigma_{X,0} = 8.5$, angular frequency $[\omega_0] = 0.1\pi$, and increasing coupling (from left to right and top to bottom): $[\lambda] = 0.25, 0.3, 0.35, 0.4$.

## 5. Acknowledgements

This work has been partially supported by Projects MTM2011–23384 and MTM2011–29342 (Ministerio de Ciencia e Innovación/FEDER, Spain), as well as FQM–316 (Junta de Andalucía).

## Appendix A. Adimensionalization

Here we review the main steps leading to the adimensionalization of our problem. To that aim, we write $w(t,x,\xi) = w^\star \widetilde{w}(\widetilde{t},\widetilde{x},\widetilde{\xi})$ with

$$t = t^\star \widetilde{t}, \quad x = L^\star \widetilde{x}, \quad \xi = v^\star \widetilde{\xi}, \tag{47}$$

where the symbols $^\star$ and $\widetilde{\ }$ have been used to denote the referential magnitudes and the dimensionless variables, respectively. Furthermore, for an external real–valued potential $V(t,x) = V^\star \widetilde{V}(\widetilde{t},\widetilde{x})$, the associated pseudo–differential operator can be expressed in function of the dimensionless variables as $\theta_V(w)(t,x,\xi) = \frac{V^\star}{mL^\star v^\star} w^\star \widetilde{\theta_V}(\widetilde{w})(\widetilde{t},\widetilde{x},\widetilde{\xi})$, where

$$\widetilde{\theta_V}(\widetilde{w})(\widetilde{t},\widetilde{x},\widetilde{\xi}) = \frac{1}{2\pi}\int_{\mathbb{R}^2} \widetilde{\delta V}(\widetilde{t},\widetilde{x},z)\widetilde{w}(\widetilde{t},\widetilde{x},\widetilde{\xi}')\, \mathrm{e}^{i\,(\widetilde{\xi}-\widetilde{\xi}')\frac{z}{mL^\star v^\star}}\, d(\widetilde{\xi}',z)\,,$$

and the rescaled symbol of the pseudo–differential operator is given by

$$\widetilde{\delta V}(\widetilde{t},\widetilde{x},z) = \frac{1}{\hbar}\left[\widetilde{V}\left(\widetilde{x}+\frac{\hbar z}{2\big(mL^\star v^\star\big)^2}\right) - \widetilde{V}\left(\widetilde{x}-\frac{\hbar z}{2\big(mL^\star v^\star\big)^2}\right)\right].$$

Then, when writing the derivatives of $w$ in terms of $\widetilde{t}$, $\widetilde{x}$ and $\widetilde{\xi}$, we are led to

$$\begin{aligned}
&\widetilde{w}_{\widetilde{t}} + \frac{v^\star t^\star}{L^\star}\widetilde{\xi}\,\widetilde{w}_{\widetilde{x}} + \frac{t^\star V^\star}{mL^\star v^\star}\widetilde{\theta_V}(\widetilde{w}) = \widetilde{\mathcal{L}_{QFP}}(\widetilde{w})\,,\\
&\widetilde{\mathcal{L}_{QFP}}(\widetilde{w})(\widetilde{t},\widetilde{x},\widetilde{\xi}) = \frac{D_{pp}t^\star}{m^2v^{\star 2}}\widetilde{w}_{\widetilde{\xi}\widetilde{\xi}} + 2\lambda t^\star\big(\widetilde{\xi}\widetilde{w}\big)_{\widetilde{\xi}} + \frac{2D_{pq}t^\star}{mL^\star v^{\star 2}}\widetilde{w}_{\widetilde{x}\widetilde{\xi}} + \frac{D_{qq}t^\star}{(L^\star)^2}\widetilde{w}_{\widetilde{x}\widetilde{x}}\,,
\end{aligned}$$

which is the dimensionless Wigner–Fokker–Planck equation (DWFPE). It is noticeable the fact that this equation is no longer influenced by $w^\star$ due to cancellation effects. Now we choose the referential magnitudes according to the peculiarities of our problem, namely

$$L^\star = \frac{\hbar}{\sqrt{6mk_BT}} \approx \lambda_{dB}\,, \quad t^\star = \frac{1}{2\lambda}\,, \quad v^\star = \frac{L^\star}{t^\star}\,,$$

representing space, time and velocity, respectively. In our framework, the typical length is conveniently chosen to be of the same order of the thermal de Broglie wavelenght, while the momentum relaxation time is normalized to unity. With these values and taking into account the definitions in (3), the DWFPE reads

$$\widetilde{w}_{\widetilde{t}} + \widetilde{\xi}\,\widetilde{w}_{\widetilde{x}} + [V^\star]\widetilde{\theta_V}(\widetilde{w}) = [D_{pp}]\widetilde{w}_{\widetilde{\xi}\widetilde{\xi}} + \big(\widetilde{\xi}\widetilde{w}\big)_{\widetilde{\xi}} + [D_{pq}]\widetilde{w}_{\widetilde{x}\widetilde{\xi}} + \frac{1}{2}\widetilde{w}_{\widetilde{x}\widetilde{x}}\,, \tag{48}$$

where

$$[V^\star] = \frac{3k_BT}{2\hbar^2\lambda^2}V^\star\,, \quad [D_{pp}] = \frac{3}{2}\left(\frac{k_BT}{\hbar\lambda}\right)^2\,, \quad [D_{pq}] = \frac{\Omega}{2\pi\lambda}\,. \tag{49}$$

Since $\frac{k_B}{\hbar} = O(10^{11})$, we are called to deal with

$$\lambda = 10^{12}[\lambda]\,, \quad \Omega = 10^{12}[\Omega]\,, \quad T = 10[T]\,, \tag{50}$$

in order to work with $O(1)$ magnitudes. Note that all of the parameters written between brackets are already dimensionless, yielding Eq. (38) up to notational simplifications.

In the particular case of $V(x) = \frac{1}{2}m\omega_0^2x^2$ we can write $V(x) = V^\star\widetilde{V}(\widetilde{x})$, where $V^\star = m\omega_0^2L^{\star 2}$ and $\widetilde{V}(\widetilde{x}) = \frac{1}{2}\widetilde{x}^2$. Thus

$$[V^\star] = \frac{\omega_0^2}{4\lambda^2} = \frac{[\omega_0]^2}{4[\lambda]^2}\,, \tag{51}$$

where we have considered $\omega_0 = 10^{12}[\omega_0]$ according to the orders of magnitude established in (50). These relations have been employed in Section 4.

In the Schrödinger scope, when taking $\Phi(t,x) = \Phi^\star\widetilde{\Phi}(\widetilde{t},\widetilde{x})$ (cf. (47)), the LSE given by (25) is now written as

$$i\widetilde{\Phi}_{\widetilde{t}} = -\frac{\alpha t^\star}{2mL^{\star 2}}\widetilde{\Phi}_{\widetilde{x}\widetilde{x}} + \frac{V^\star t^\star}{\alpha}\widetilde{V}\widetilde{\Phi} + \frac{t^\star\Lambda}{\alpha}\log(n_{\widetilde{\Phi}})\widetilde{\Phi} + \frac{t^\star\Lambda}{\alpha}\log(|\Phi^\star|^2)\widetilde{\Phi}\,,$$

as shed from simple computations. Since we are interested in the observable behaviour, we may perform the following change of global phase

$$\widetilde{\Phi} \longmapsto \exp\big\{-i\log(|\Phi^\star|^2)t\big\}\widetilde{\Phi}$$

and obtain

$$i\widetilde{\Phi}_{\widetilde{t}} = -\frac{1}{2}\widetilde{\Phi}_{\widetilde{x}\widetilde{x}} + [V^\star]\widetilde{V}\widetilde{\Phi} + [\Lambda]\log(n_{\widetilde{\Phi}})\widetilde{\Phi} \tag{52}$$

with $[\Lambda] = \frac{1}{2} + [D_{pq}]$, which is Eq. (44) up to notational simplifications.

## Appendix B. The numerical scheme

We give here a short description of the numerical procedure employed to approximate the standard deviation of the solution to the 1D initial value problem associated with Eq. (44), to be compared with that corresponding to the exact Wigner–Fokker–Planck solution as established in Section 4. Specifically, we are concerned with an adaptation of the conservative scheme introduced in [34] to our situation.

Consider the interval $[a,b]$ and the following partition of $\mathbb{R}_0^+ \times [a,b]$, with time step $dt > 0$ and length interval $dx = (b-a)/n$, $n \in \mathbb{N}$:

$$\mathcal{U} = \big\{(t^j, x_l) \in \mathbb{R}_0^+ \times [a,b] : \, j = 0,1,2,\ldots,\ l = 0,1,\ldots,n\big\}\,,$$

where

$$t^j = j\,dt \quad \forall j = 0, 1, 2, \dots \text{ and } x_l = a + l\,dx \quad \forall l = 0, 1, \dots, n\,.$$

We also denote $u_l^j := u(t^j, x_l)$ for all $j = 0, 1, \dots$ and $l = 0, \dots, n$, $u$ being any function defined on the grid $\mathcal{U}$.

In order to evaluate the spacial derivatives we choose centered differences, so that the Laplacian of $u$ will be approximated in terms of the usual formula:

$$u_{xx}(x_l) \approx \frac{u(x_{l+1}) - 2u(x_l) + u(x_{l-1})}{(dx)^2}\,, \quad l = 0, 1, \dots, n\,.$$

It is remarkable that this equality also holds for the extremal points, given that null boundary conditions are imposed at infinity (so that $x_{-1} = x_{n+1} = 0$). Now, we consider the discrete operators

$$\delta_t u^j = \frac{u^{j+1} - u^j}{dt}\,, \quad \mu_t u^j = \frac{1}{2}\big(u^{j+1} + u^j\big)\,, \quad j = 0, 1, \dots$$

for any $u$ defined on $\mathcal{U}$. Then, the discretized version of Eq. (44) reads

$$i\delta_t \Phi_l^j + \frac{1}{2}\mu_t(\Phi_l^j)_{xx} - \mu_t U_l^j \mu_t \Phi_l^j = 0\,, \tag{53}$$

where we denoted $\Phi$ the numerical approximation to be provided by our scheme, and where $U$ embraces the external potential as well as the nonlinearity:

$$U_l^j = [V^\star]V_l^j + [\Lambda](\log n)_l^j\,. \tag{54}$$

Observe that Eq. (53) entails a complicated nonlinear system, whose numerical solvability constitutes a serious drawback. In order to overcome this difficulty we invoke a predictor–corrector procedure $\Phi^j \mapsto \Phi^{j,1} \mapsto \Phi^{j+1}$, where the prediction step $\Phi^{j,1}$ is attained by solving the following difference equation

$$i\,\frac{\Phi_l^{j,1} - \Phi_l^j}{dt} + \frac{1}{4}\big((\Phi_l^{j,1})_{xx} + (\Phi_l^j)_{xx}\big) - \frac{1}{2}U_l^j\big(\Phi_l^{j,1} + \Phi_l^j\big) = 0\,. \tag{55}$$

Then, according to (54) we may construct

$$U_l^{j,1} = [V^\star]V_l^{j,1} + [\Lambda](\log n)_l^{j,1}\,,$$

and finally solve

$$i\,\frac{\Phi_l^{j,2} - \Phi_l^j}{dt} + \frac{1}{4}\big((\Phi_l^{j,2})_{xx} + (\Phi_l^j)_{xx}\big) - \frac{1}{4}\big(U_l^{j,1} + U_l^j\big)\big(\Phi_l^{j,2} + \Phi_l^j\big) = 0\,. \tag{56}$$

The correction step is then defined as $\Phi^{j+1} := \Phi^{j,2}$. It is noticeable the fact that this scheme is mass–preserving, which reveals of crucial importance in our framework (cf. (i) in Lemmata 1 and 2).

To close this section we observe that, in order to avoid singularities, the discretization of the logarithmic term is implemented in such a way that $\big(\log n\big)_l^j$ is truncated as $\log(\mathrm{TOL})$ whenever $n_l^j < \mathrm{TOL}$, with $\mathrm{TOL} = 10^{-20}$.

## References


[1] A. Arnold, J. L. López, P. A. Markowich and J. Soler, *An analysis of quantum Fokker–Planck models: a Wigner function approach*, Rev. Mat. Iberoamericana, **20** (2004), 771–814.

[2] Auberson, G., Sabatier, P. C. *On a class of homogeneous nonlinear Schrödinger equations*, J. Math. Phys. **35**(8) (1994), 4028–4040.

[3] Bialynicki–Birula, I., Mycielski, J. *Nonlinear wave mechanics*, Ann. Phys. **100** (1996), 62–93.

[4] Caldeira, A. O., Leggett, A. J. *Path integral approach to quantum Brownian motion*, Physica A **121** (1983), 587–616.

[5] Cazenave, T. *Stable solutions of the logarithmic Schrödinger equation*, Nonlinear Analysis T. M. A. **7** (1983), no. 10, 1127–1140.

[6] Cazenave, T., Haraux, A. *Equations d'évolution avec non linéarité logarithmique*, Annals Fac. Sci. Univ. Toulouse **2** (1980), 21–55.

[7] Cufaro Petroni, N., De Martino, S., De Siena, S., Illuminati, F. *Stochastic–hydrodynamic model of halo formation in charged particle beams*, Phys. Rev. ST Accel. Beams **6** (2003), 034206.

[8] Davidson, M. P. *Comments on the nonlinear Schrödinger equation*, Il Nuovo Cimento B **V116B** (2001), 1291–1296.

[9] Davis, E. B. *Quantum theory of open systems* (Academic, London, 1976).

[10] Dekker, H., Valsakumar, M. C. *A fundamental constraint on quantum mechanical diffusion coefficients*, Phys. Lett. **104A** (1984), no. 2, 67–71.

[11] De Martino, S., Lauro, G. *Soliton–like solutions for a capillary fluid*, Waves and Stability in Continuous Media, Proceedings of the 12th Conference on WASCOM 148–152 (2003).

[12] De Martino, S., Falanga, M., Godano, C., Lauro, G. *Logarithmic Schrödinger–like equation as a model for magma transport*, Europhys. Lett. **63** (2003), no. 3, 472–475.

[13] Diósi, L. *Caldeira–Leggett master equation and medium temperatures*, Physica A **199** (1993), 517–526.

[14] Doebner, H. D., Goldin, G. A. *On a general nonlinear Schrödinger equation admitting diffusion currents*, Phys. Lett. A **162** (1992), 397–401.

[15] Gao, S. *Dissipative quantum dynamics with a Lindblad functional*, Phys. Rev. Lett. **79** (1997), no. 17, 3101–3104.

[16] Garbaczewski, P. *Modular Schrödinger equation and dynamical duality*, Phys. Rev. E **78** (2008), 031101.

[17] Gardner, C. *The quantum hydrodynamic model for semiconductor devices*, SIAM J. Appl. Math. **54** (1994), 409–427.

[18] Guerra, F. *Structural aspects of stochastic mechanics and stochastic field theory*, Phys. Rep. **77** (1981), no. 3, 263–312.

[19] Guerrero, P., López, J. L., Nieto, J. *Global $H^1$ solvability of the 3D logarithmic Schrödinger equation*, Nonlinear Analysis: Real World Applications **11** (2012), 79–87.

[20] Guerrero, P., López, J. L., Montejo–Gámez, J., Nieto, J. *Wellposedness of a nonlinear, logarithmic Schrödinger equation of Doebner–Goldin type modeling quantum dissipation*, J. Nonlinear Science **22** (2012), 631–663.

[21] Jüngel, A., López, J. L., Montejo–Gámez, J. *A new derivation of the quantum Navier–Stokes equations in the Wigner–Fokker–Planck approach*, J. Stat. Phys. **145** (2011), 1661–1673.

[22] Kossakowski, A. *On necessary and sufficient conditions for a generator of a quantum dynamical semi–group*, Bull. Acad. Pol. Sci., Ser. Sci. Math. Astr. Phys. **20** (1972), no. 12, 1021–1025.

[23] Kostin, M. D. *On the Schrödinger–Langevin equation*, J. Chem. Phys. **57**, 3589–3591 (1972); *Friction and dissipative phenomena in quantum mechanics*, J. Stat. Phys. **12** (1975), 145–151.

[24] Lauro, G. *A note on a Korteweg fluid and the hydrodynamic form of the logarithmic Schrödinger equation*, Geophys. and Astrophys. Fluid Dynamics **102** (2008), no. 4, 373–380.

[25] Lindblad, G. *On the generators of quantum dynamical semigroups*, Comm. Math. Phys. **48** (1976), 119–130.

[26] López, J. L. *Nonlinear Ginzburg–Landau–type approach to quantum dissipation*, Phys. Rev. E. **69** (2004), 026110.

[27] López, J. L., Montejo–Gámez, J. *A hydrodynamic approach to multidimensional dissipation-based Schrödinger models from quantum Fokker-Planck dynamics*, Physica D **238** (2009), no. 6, 622–644.

[28] López, J. L., Montejo–Gámez, J. *On viscous quantum hydrodynamics associated with nonlinear Schrödinger–Doebner–Goldin models*, Kinetic and related models **5** (2012), 517–536.

[29] López, J. L., Montejo–Gámez, J. *On the derivation and mathematical analysis of some quantum–mechanical models accounting for Fokker–Planck type dissipation: Phase space, Schrödinger and hydrodynamic descriptions*, Nanoscale Systems: Mathematical Modeling, Theory and Applications **2**, 49–80 (2013), ISSN (Online) 2299–3290.

[30] Madelung, E. *Quantentheorie in hydrodynamischer form*, Z. Phys. **40** (1927), 322–326.

[31] Nattermann, P., Scherer, W. *Nonlinear gauge transformations and exact solutions of the Doebner–Goldin equation*, in Nonlinear, Deformed and Irreversible Quantum Systems, Doebner *et al.* (Eds.), 188–199, World Scientific 1995.

[32] Nelson, E. *Derivation of the Schrödinger equation from Newtonian Mechanics*, Phys. Rev. **150** (1966), 1079–1085.

[33] Pollak, E., Zhang, S. *Quantum dynamics for dissipative systems: A numerical study of the Wigner–Fokker–Planck equation*, J. Chem. Phys. **118** (2003), no. 10, 4357–4364.

[34] Ringhofer, C., Soler, J. *Discrete Schrödinger–Poisson systems preserving energy and mass*, Appl. Math. Lett. **13** (2000), no. 7, 27–32.

[35] Vacchini, B. *Completely positive quantum dissipation*, Phys. Rev. Lett. **84** (2000), no. 7, 1374–1377.

[36] Wallstrom, T. C. *Inequivalence between the Schrödinger equation and the Madelung hydrodynamic equations*, Phys. Rev. A (1994), no. 3, 1613–1617.

Pilar Guerrero
Centre de Recerca Matemática
Campus de Bellaterra, edifici C
Bellaterra, 08193 Barcelona, Spain

José Luis López, Jesús Montejo–Gámez
Departamento de Matemática Aplicada
Facultad de Ciencias
Universidad de Granada
18071 Granada, Spain